

Angular momentum dependence of photoionization cross sections from the excited states of lithium

Shahid Hussain, M. Saleem, and M. A. Baig*

Atomic and Molecular Physics Laboratory, Department of Physics, Quaid-i-Azam University, Islamabad 45320, Pakistan

(Received 15 August 2006; published 6 November 2006)

We present new measurements of photoionization cross sections from the $4s\ ^2S$, $4p\ ^2P$, and $4d\ ^2D$ excited states of lithium, above the first ionization threshold. The experiments have been conducted using two dye lasers pumped by a Nd:yttrium aluminum garnet (YAG) laser in conjunction with a thermionic diode ion detector and pump-probe saturation technique. The behavior of the photoionization cross sections from $n=4$ and $l=0, 1, 2$ excited states have been investigated. A smooth wavelength dependence of photoionization cross sections has been observed for the $4p$ and $4d$ excited states, which decrease monotonically with the decrease in the ionizing laser wavelength; however, the falloff for the $4d$ excited state is purely hydrogenic. The cross section for the $4s$ excited state first increases, attains a maximum value, and then decreases monotonically with a decrease in the ionizing wavelength—strictly nonhydrogenic. The measured values of the cross section are compared with the earlier theoretical work.

DOI: [10.1103/PhysRevA.74.052705](https://doi.org/10.1103/PhysRevA.74.052705)

PACS number(s): 32.80.Fb, 32.80.Rm, 32.80.Cy

I. INTRODUCTION

Lithium is the simplest element after hydrogen and helium, and the description of its valence electron is particularly simple as the electron moves in the coulomb field of the nuclear charge shielded by the two closed K shell electrons. The electron correlation effects can also be neglected and the main modification to the asymptotic coulomb potential is produced by the core polarization. Therefore, it is an important atom to study photon-atom interaction and in particular the photoionization processes. Photoionization is the simplest process providing detailed information on the atomic and molecular structure. The photoionization from the ground state of many atoms has been studied extensively [1,2] but comparatively less is known about the photoionization of the excited states, although it is of great importance in the controlled thermonuclear and in the extremely hot stellar atmosphere research.

Apart from a few early attempts [3,4], the knowledge of the photoionization cross sections of the excited states of lithium, especially of the energy-dependent cross section, has progressed only by theoretical efforts. Aymar *et al.* [5] computed the photoionization cross section for the s , p , and d Rydberg states of Li in the framework of a single-electron model by using a parametric central potential and compared their results with other theoretical work [6–8]. Barrientos and Martin [9] applied the quantum defect orbital method to compute the oscillator strength and photoionization cross sections of lithium. Lahiri and Manson [10] calculated the radiative-recombination rate coefficients for the electrons impinging on Li^+ , along with the associated excited-state photoionization cross sections in the low-energy region. A brief review of the theory and the relationship between the photoionization and the recombination was also presented. Chung [11] calculated the 2S and 2D photoionization cross section of lithium from the $2p$ state for photon energies below the $\text{Li}^+ 1s2s\ ^1S$ ionization threshold.

Different experimental techniques have been used for the measurements of the photoionization cross sections of the excited states. Rothe [3] pioneered the studies on the photoionization of the excited states of lithium based on the radiative electron-ion recombination and shock-heated plasma and determined the photoionization cross section for the $2p$ excited state at threshold as 19.7 Mb. Kramer *et al.* [12] studied the resonant three-photon ionization process of lithium and measured the photoionization cross section at 610.4 nm using the saturation technique. Wippel *et al.* [13] used the magneto-optical trap to determine the photoionization cross sections of the excited states of sodium and lithium (^7Li and ^6Li) at different ionizing laser wavelengths. They reported the cross section of the $2p$ excited state of lithium at 334.47 nm and 335.85 nm above the first ionization threshold. Recently, Saleem *et al.* [14] proposed an alternate technique for the measurement of the photoionization cross sections of the excited states of the isotopic atoms.

In this work, we present an experimental determination of the photoionization cross sections from the $4s\ ^2S$, $4p\ ^2P$, and $4d\ ^2D$ excited states of lithium. Four different regions of the continuum, above the first ionization threshold, have been investigated corresponding to each of the three excited states. The photoionization cross sections have been determined at the ionizing wavelengths of 1064 nm, 690 nm, 532 nm, and 317 nm. The energy-dependent behavior of the photoionization cross is also discussed.

II. EXPERIMENTAL SETUP

A schematic of the experimental arrangement for the measurement of the photoionization cross section from the excited states of lithium is shown in Fig. 1. The laser system comprised of a Q -switched pulsed Nd:yttrium aluminum garnet (YAG) laser (Brilliant B, Quantel) coupled with the second-harmonic generation (SHG) module for producing laser at 532 nm with the corresponding energy of 450 mJ. It operates at 10 Hz with pulse duration of ≈ 5 ns. The 90% of the laser energy at 532 nm was used to pump a commercial dye laser system (Quantel, TDL-90), while the remaining 10% was used to pump a homemade Hanna-type dye laser

*Corresponding author. FAX: +92 51 9210256. Email address: baig@qau.edu.pk

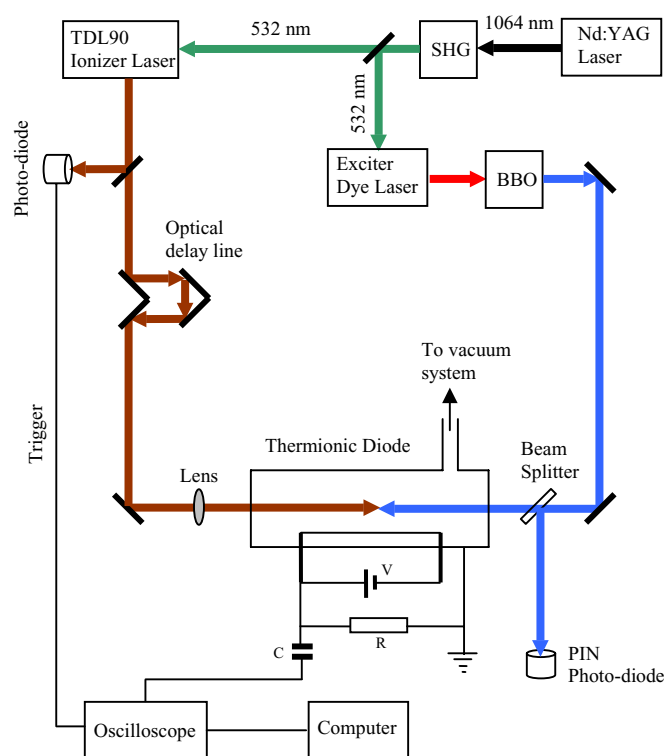


FIG. 1. (Color online) Schematic diagram of the experimental setup for two-step photoionization of lithium.

cavity [15]. The cavity was formed between a flat mirror and a 2400 lines/mm holographic grating, and the wavelength tuning was achieved by rotating the grating with a computer-controlled stepper motor. The linewidth of the TDL-90 dye laser was $\leq 0.1 \text{ cm}^{-1}$ whereas that of Hanna type was $\leq 0.3 \text{ cm}^{-1}$. The dye laser wavelength was determined by a spectrometer (Ocean Optics, HR2000) equipped with a 600 lines/mm grating. The intensity of the ionizing laser was varied by inserting the neutral density filters (Edmund Optics), and on each insertion the energy was measured by an energy meter (R-752, Universal Radiometer).

The lithium vapors were produced in a thermionic diode ion detector composed of a stainless steel tube 48 cm long, 3 cm in diameter, and 1 mm wall thickness. About 20 cm of the central part of the tube was placed in a clamp-shell oven. Both ends of the tube were water-cooled and sealed with 25 mm diameter quartz windows. The thermionic diode was then heated up to 800 K corresponding to a lithium vapor pressure of 0.01 Torr. The temperature was monitored by a Ni-Cr-Ni thermocouple and it was maintained within $\pm 1\%$ by a temperature controller. A molybdenum wire 0.25 mm in diameter stretched axially, heated by a separate regulated dc power supply, served as a cathode for the ion detection. About 2 g of spectroscopically pure lithium was placed at the central heating zone of the tube. The tube was evacuated up to 10^{-6} Torr and subsequently filled with argon gas at about 0.2 Torr, which serves as a buffer gas and provides a uniform column of the lithium vapors and also protects the quartz windows from the metallic coatings. The ionization signals were registered as a change in the voltage across a load resistor. The variation in the amplitude of the ionization

signal with the laser intensity was recorded using a 200 MHz digital storage oscilloscope (TDS 2024) and a computer through RS232 interface.

The homemade dye laser, pumped by the 532 nm, charged with R-590 and fluoresceine 548 dyes dissolved in methanol and tuned at 571.2 nm and 546.1 nm, was used to populate respectively the $4s^2S$ and $4d^2D$ excited states via two-photon excitation. The dye laser charged with fluoresceine 548 dye, tuned at 548.4 nm and frequency doubled with the beta-barium-borate (BBO) crystal, was used to populate the $4p^2P$ excited level at 273.05 nm. The excited atoms from the $4s$, $4p$, and $4d$ states were then photoionized by the laser at 1064 nm (fundamental of Nd:YAG laser), 690 nm, 532 nm (second harmonic), and 317 nm. The wavelength at 690 nm was achieved by charging the TDL-90 dye laser with [2-[4-[4-(dimethylamino)phenyl]-1,3-butadienyl]-1-ethylpyridinium monoperchlorate (LDS-698) dissolved in methanol. For the 317 nm wavelength, the TDL-90 dye laser was charged with [2-[2-[4-(dimethylamino)phenyl]ethenyl]-6-methyl-4H-pyran-4-ylidene]-propanedinitrile (DCM) dissolved in methanol and then frequency doubled by the BBO crystal. Both the laser pulses were linearly polarized with parallel polarization axis. The two laser beams (the exciter and the ionizer), entering the thermionic diode from the opposite sides, overlap at its center. The relative delay between the exciter and the ionizer laser pulses was controlled and varied by an optical delay line. The temporal overlap of both the laser pulses was checked using a fast PIN photodiode (BPX 65).

III. RESULTS AND DISCUSSION

The two-step excitation/ionization scheme for the measurement of the photoionization cross sections of the excited states of lithium is shown in Fig. 2. In the first step, the lithium atoms were optically excited from the ground state to the $4s^2S$, $4p^2P$, and $4d^2D$ excited states. In the second step, the excited electrons were promoted to the $\text{Li}^+ 1s^2 1S$ continuum by four different laser pulses at 1064 nm, 690 nm, 532 nm, and 317 nm. The ionizing lasers, having different wavelengths, produce electrons of different kinetic energies, and four different regions of the continuum are investigated corresponding to each of the three excited states. Since only one continuum ($\text{Li}^+ 1s^2 1S$) can be reached with the laser energies used, the number of electrons produced are equivalent to the number of Li^+ ions and hence the ionization signal directly reflects the photoionization cross section.

The $4s^2S_{1/2}$ excited state of lithium has no fine structure splitting due to the spin-orbit interaction and is populated via two-photon excitation from the ground state. The $4p^2P_{1/2,3/2}$ excited states, at $36469.714 \text{ cm}^{-1}$ and $36469.754 \text{ cm}^{-1}$ [16] are populated by absorbing a single photon at 273.05 nm from the ground state of lithium. Since the laser line width ($\sim 0.3 \text{ cm}^{-1}$) of our system is greater than the fine structure splitting ($\sim 0.04 \text{ cm}^{-1}$) in the $4p$ states, therefore both the $4p^2P_{1/2}$ and $4p^2P_{3/2}$ states are populated. Hence we were unable to determine the photoionization cross sections of $4p^2P_{1/2}$ and $4p^2P_{3/2}$ excited states separately. The even parity $4d^2D_{3/2,5/2}$ states, at $36623.297 \text{ cm}^{-1}$ and $36623.312 \text{ cm}^{-1}$ respectively [16], were populated via two-

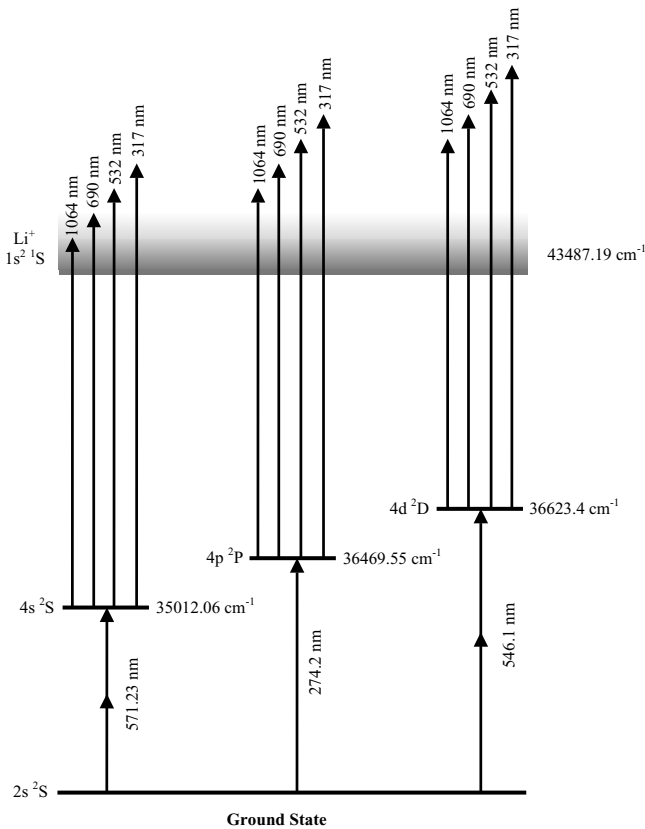


FIG. 2. Energy level diagram for the measurement of photoionization cross section from the $4s$, $4p$, and $4d$ excited states of lithium. The level energies are taken from NIST data [16].

photon excitation process from the ground state. As the fine structure splitting in the $4d$ states is 0.015 cm^{-1} , it could not be resolved in the present work. Therefore, both the $4d \ ^2D_{3/2}$ and $4d \ ^2D_{5/2}$ states are populated. Hence, in the present work the measured value of the photoionization cross sections from the $4d$ excited state at different ionizing laser wavelengths contains the contributions of both the $^2D_{3/2}$ and $^2D_{5/2}$ fine structure components.

The saturation technique pioneered by Ambartzumian *et al.* [17] was used to determine the absolute photoionization cross sections of the excited states of lithium. This technique has been widely used for the measurement of the photoionization cross sections of the excited states of alkali atoms, alkaline earths, and rare gas atoms [18–25]. Burkhardt *et al.* [26] applied this technique to measure the absolute cross section from the excited states of sodium, potassium, and barium. He *et al.* [27] reported the absolute photoionization cross section of the $6s6p \ ^1P_1$ excited state of barium using the same technique. Similar method has been used by Xu *et al.* [28] to measure the absolute photoionization cross sections of the autoionizing states of lutetium. We have also used this technique for the measurement of the photoionization cross section and the optical oscillator strength of the autoionization resonances in neon using a hollow cathode dc discharge [29]. Amin *et al.* [30,31] applied the saturation method to determine the photoionization cross sections of excited states of sodium and lithium using a thermionic diode ion detector. Recently, we have applied this

technique to measure the absolute photoionization cross section from $3p \ ^1,^3P$ excited states of helium using a dc discharge [32].

As a result of two-step photoionization process, ions are produced that are detected as a voltage across a load resistor. The collected charge Q per pulse in terms of this voltage signal is given as

$$Q = \left(\frac{\text{Voltage signal}}{R} \right) \times \Delta t. \quad (1)$$

Here R is the load resistance and Δt is the full width at half maximum pulse width of the photoion signal peak in seconds.

In the absence of collisions and ignoring the spontaneous emission, for a pure two-step photoionization process, the rate equations have been solved to find a relation between the total charge per pulse and the photoionization cross section [26] as

$$Q = eN_0V_{vol} \left[1 - \exp\left(-\frac{\sigma U}{2\hbar\omega A}\right) \right]. \quad (2)$$

Here e is the electronic charge, N_0 is the density of the excited atoms, A is the cross-sectional area of the ionizing laser beam, U is the total energy per pulse of the ionizing laser, V_{vol} is the interaction volume, and σ is the absolute cross section for photoionization. This equation holds with the assumption that the intensity of the ionizing laser is higher, i.e., in access to that required for saturating the resonance transition; also, the transition remains saturated during the laser pulse and the laser beam is uniform and linearly polarized.

All quantities in Eq. (2) are either known or can be measured except the number density N_0 and the cross section σ . These quantities can be determined by least-square fitting to the plot of Q versus U . It is evident that as $U \rightarrow \infty$, $Q \rightarrow eN_0V$, i.e., the determination of N_0 is independent of the photoionization cross section. The cross section σ is associated with the shape of the Q versus U plot. The accurate value of N_0 can only be extracted if the amplification of the thermionic diode detector is known. The accurate measurement of the photoionization cross section σ depends upon the accuracy with which the energy of the ionizing laser (U) and the cross-sectional area (A) of the laser beam are measured. The uncertainty in the energy determination is mostly owing to the energy fluctuations in the Nd:YAG laser ($\pm 5\%$) and in the energy measuring instrument ($\pm 3\%$).

The thermionic diode is a very sensitive ion detector, having an amplification factor of 10^4 – 10^6 or even larger and is an excellent tool for the study of highly excited Rydberg states of atoms and molecules [33]. The linearity of the detector is very important while recording the experimental data of the photoionization signals so that an actual change of the photoions signal versus the energy density of the ionizer laser can be registered. We configured the linearity of our detector for the strongest photoion signal corresponding to the maximum available ionizing laser intensity. For this purpose we have tried different combinations of the coupling capacitor “C” and the load resistor “R” as shown in Fig. 1. It was found that shape of the optogalvanic voltage signal

changes significantly with the value of the load resistor. The values of “R” and “C” were adjusted to avoid the saturation of the electronics and to record the pure photoion signals.

Equation (2) reflects that the extraction of photoionization cross sections strongly depends on the area of cross section of the ionizing laser in the interaction region. The diameter of the exciter laser was ≈ 3 mm, which passes through the center of the thermionic diode ion detector. An aperture was placed in the path of the ionizing laser to confine its diameter to ≈ 2 mm. To characterize the exciting and the ionizing laser’s spatial profile, two beam splitters were placed before the entrance of the thermionic diode and a small fraction of the exciter and the ionizer laser beams was used to reproduce their spatial profiles at the interaction region. The spatial profiles of both exciter and ionizer lasers were generated by scanning a PIN photodiode across their diameters. The intensity distribution of both the laser beams was found to be Gaussian. Their spot sizes were determined at which the irradiance (intensity) falls to $1/e^2$ of its axial value. Since the diameter of the ionizer laser beam was smaller than that of the exciter laser, it therefore reduces the problems associated with the spatial overlap of the beams.

We have sufficient laser energy at 1064 nm to saturate the $4s$, $4p$, and $4d$ excited states of lithium. A lens of focal length 50 cm was used for the ionizing lasers of wavelength 690 nm, 532 nm, and 317 nm to meet the power requirements for the saturation. The area of the overlap region in the confocal limit is calculated using the following relation [34,35]

$$A = \pi\omega_0^2 \left[1 + \left(\frac{\lambda_{io}z}{\pi\omega_0^2} \right)^2 \right]. \quad (3)$$

Here z is the distance on the beam propagation axis from the focus, $\omega_0 = f\lambda_{io}/\pi\omega_s$ is the beam waist at $z=0$, ω_s is half the spot size of the ionizing laser beam on the focusing lens, f is the focal length, and λ_{io} is the wavelength of the ionizing laser.

The $4s^2S$, $4p^2P$, and $4d^2D$ excited states have much greater lifetimes $\{\tau(4s) \approx 57.24$ ns [10], $\tau(4p) \approx 424.85$ ns [10], and $\tau(4d) = 33.5$ ns [10] $\}$ than the linewidth of both the exciter and the ionizer laser. Therefore, in order to separate the excitation and the ionization steps and to ensure a pure two-step photoion signal, the ionizing laser was delayed by ≈ 5 ns. The amplitudes of the photoion signals are plotted as a function of the intensity of the ionizing laser. Typical experimental curves for the $4s^2S$, $4p^2P$, $4p^2D$ excited states of lithium at 1064 nm are presented in Fig. 3. The solid lines that pass through the experimental data points are the least-squares fit to Eq. (2). It is evident that the photoion signal first increases linearly with the ionizing laser’s intensity and then saturates; i.e., the photoion signal stops to increase by further increase in the ionizing laser intensity. The threshold intensity of the ionizing laser at which the saturation just sets is relatively lower for $4p$ and $4d$ while a higher intensity is required to ionize the $4s$ excited state. This difference in the threshold intensity is attributed to the corresponding photoionization cross sections. For a higher value of cross section, the photoion signal gets saturated at very low ionizing laser intensity. The photoionization cross sections from the three

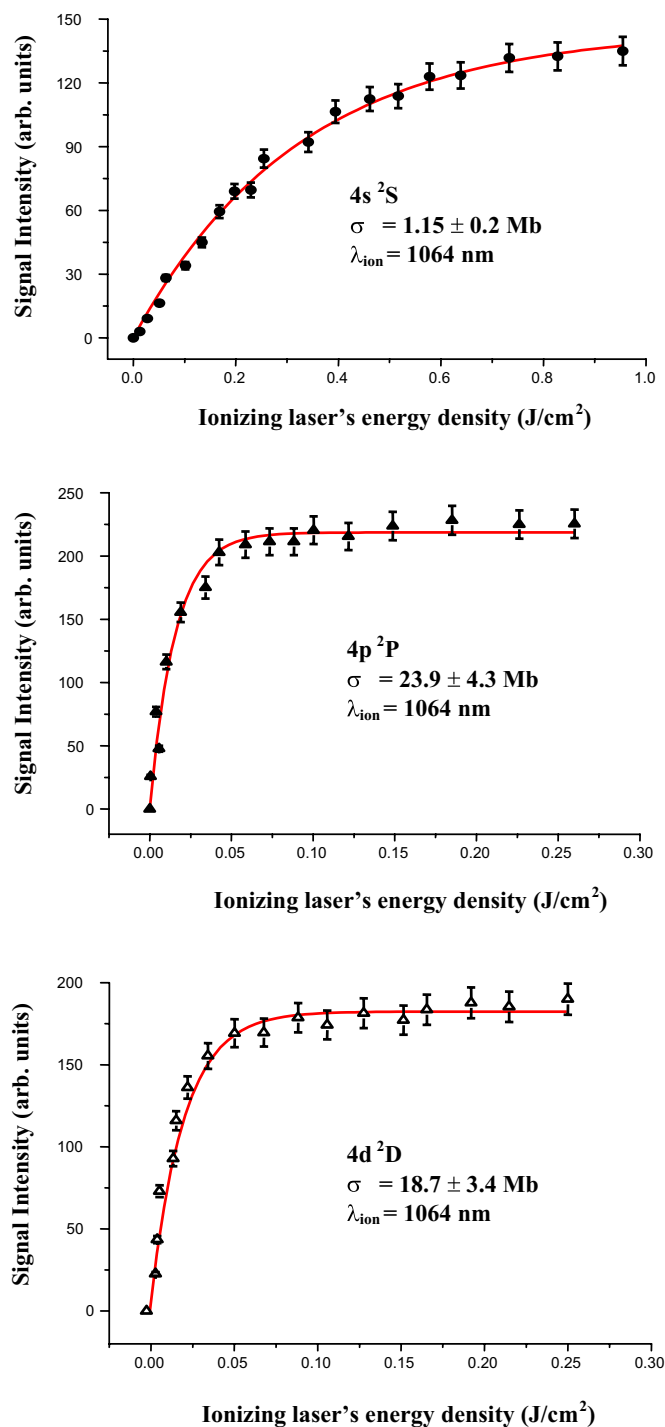


FIG. 3. (Color online) The photoionization data for the $4s^2S$, $4p^2P$, and $4d^2D$ excited states of lithium with the ionizing laser set to a wavelength of 1064 nm. The solid lines are the least squares fit to Eq. (2) to the observed data for extracting the photoionization cross section. The error limits on the data results from pulse-to-pulse fluctuations in the signal.

excited states of lithium determined from the fitting procedure, along with the earlier reported theoretical values, are summarized in Table I. The maximum overall uncertainty in the determination of the absolute cross section is estimated to be 18% [36], which is attributed to the experimental errors in

TABLE I. Experimental data for the absolute photoionization cross section from the $4s$, $4p$, and $4d$ excited states of lithium.

Present work (Experimental)			Previous work (Theoretical)
State	wavelength (nm)	Cross section (Mb)	Cross section (Mb)
$4s^2S$	1180		1.40 [5]; 1.31 [7]
	1064	1.15 ± 0.21	
	690	1.25 ± 0.23	
	532	1.03 ± 0.18	
	317	0.57 ± 0.10	
$4p^2P$	1425		41.70 [5]; 34.20 [7]
	1064	23.9 ± 4.3	
	690	8.8 ± 1.6	
	532	3.9 ± 0.7	
	317	2.0 ± 0.4	
$4d^2D$	1457		36.20 [5]; 30.60 [7]
	1064	18.7 ± 3.4	
	690	4.0 ± 0.7	
	532	1.8 ± 0.3	
	317	0.5 ± 0.1	

the measurements of the laser energy, the calibration of the detection system, and the cross-sectional area of the ionizing laser beam in the interaction region.

We have reported the experimental determination of the photoionization cross section of $4s$, $4p$, and $4d$ excited states of lithium. We can only compare our results with the theoretical work. The measured values of cross sections along with the earlier theoretical work are shown in Fig. 4. The continuous curves for $4s$ and $4p$ excited states in Figs. 4(a) and 4(b) are the work of Lahiri and Manson [10], who used the central-potential model to calculate the cross sections of excited states of lithium. The calculated values for $4s$, $4p$, and $4d$ excited states at the ionization threshold by Aymar *et al.* [5] and by Gezalov and Ivanova [7] are also shown in the Fig. 4. We have determined the cross section from the $4p$ excited state up to ≈ 3 eV above the ionization threshold, but the theoretical curve from Lahiri and Manson [10] covers the energy range from the ionization threshold up to 1.4 eV. In order to compare the results, we fitted the exponential decay law to the experimental values. The dotted line is the fitted curve and shows an excellent agreement with the theoretical work. Also, the photoionization cross section from $4p$ excited states decays smoothly with the decrease in the ionizing laser wavelength. Very little information is available about the photoionization cross section from the $4d$ excited state of lithium. Aymar *et al.* [5] calculated the photoionization cross section of $4d$ excited state at the ionization threshold as 36.2 Mb whereas Gezalov and Ivanova [7] reported its value as 30.6 Mb; no other theoretical or experimental data are available for photoionization cross section from $4d$ excited state of lithium. The measured values of the photoionization cross section of $4d$ excited state along with the values at threshold calculated by Aymar *et al.* [5] and Gezalov and Ivanova [7] are shown in Fig. 4(c). The solid line is the

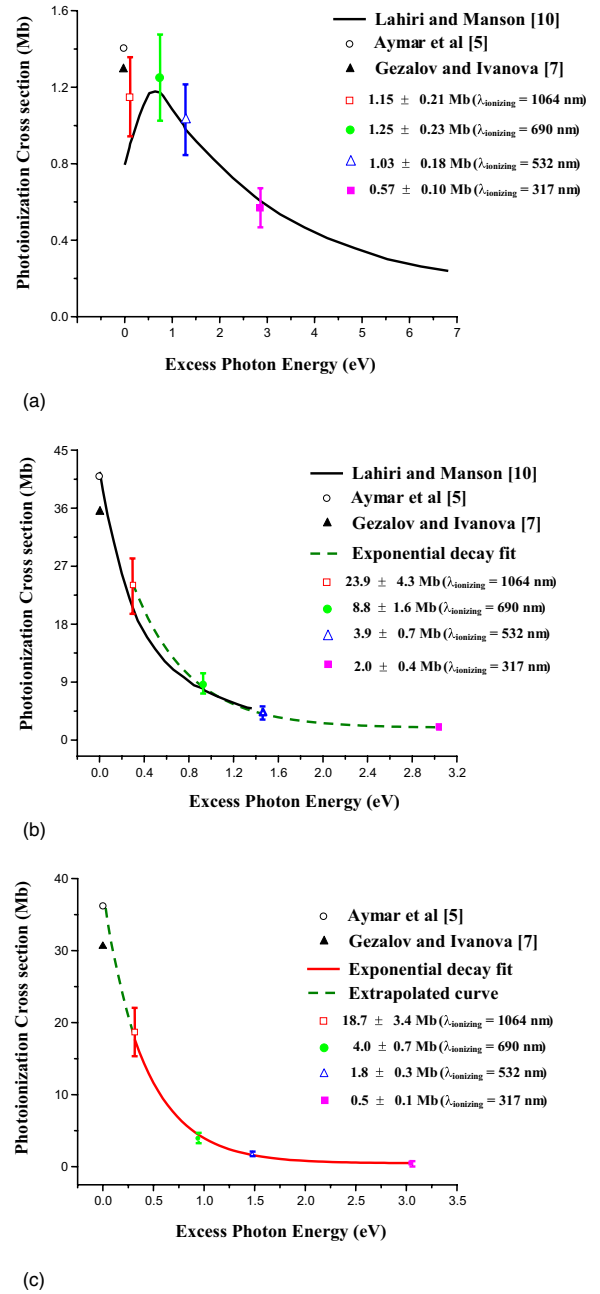


FIG. 4. (Color online) (a) Comparison of the experimentally measured values of the absolute photoionization cross section from the $4s^2S$ excited state with the theoretical work. The solid line is the calculated curve presented by Lahiri and Manson [10]. The calculated values at threshold by Aymar *et al.* [5] and by Gezalov and Ivanova [7] are also shown. (b) Comparison of the experimentally measured values of the absolute photoionization cross section from the $4p^2P$ excited state with the theoretical work. The solid line is the calculated curve presented by Lahiri and Manson [10]. The calculated values at threshold by Aymar *et al.* [5] and by Gezalov and Ivanova [7] are also shown. The dotted line is the exponential decay fit to the experimental data points. (c) The experimentally measured values of the absolute photoionization cross section from the $4d^2D$ excited state are shown along with the calculated values at threshold by Aymar *et al.* [5] and by Gezalov and Ivanova [7]. The solid line is the exponential decay fit to the experimental data points. The dotted part of the line is the extrapolation.

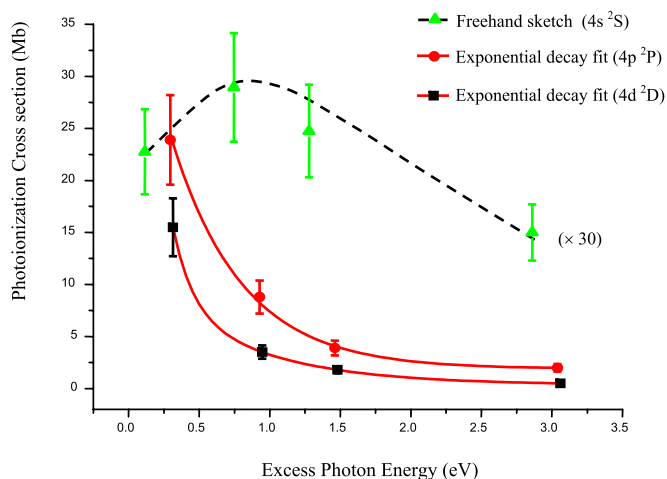


FIG. 5. (Color online) A comparison between the energy-dependent behavior of the measured values of the photoionization cross section from the $4s$, $4p$, and $4d$ excited states of lithium. The values of the photoionization cross section from the $4s$ excited state are multiplied by 30 just to show the trends of cross section from the three excited states. The dotted line passing through the values of the cross section of the $4s$ excited state is not the fitted curve, it is just a freehand sketch. The solid lines are the exponential decay fit to the experimental data points for the photoionization cross section from the $4p$ and $4d$ excited states.

exponential decay fit to the experimental data points. The extrapolation of this line gives the threshold photoionization cross section of the $4d$ excited state very close to the calculated values [5,7]. The dotted line is the extrapolated part of the fitted curve.

The measured values of the photoionization cross section for the three excited states are collectively presented in Fig. 5. The values of cross section from the $4s$ excited state are multiplied by a factor of 30 just to compare the trends of photoionization cross sections from the three excited states. The dotted line passing through the values of the cross section of the $4s$ excited state at different ionizing wavelengths is not the fitted curve; it is just a freehand sketch to compare the trend of the energy dependence of the photoionization cross section from the three excited states corresponding to the same principal quantum number but different orbitals. The solid lines are the exponential decay fit to the experimental data points for the photoionization cross section from $4p$ and $4d$ excited states.

The behavior of the photoionization cross sections for the excited states can be correlated with the difference between the initial state quantum defect and the final continuum threshold phase shift. The quantum defects of s and p states of lithium are 0.4 and 0.05 respectively and are effectively zero for $\ell \geq 2$ [10]. Thus only transitions involving s or p states are nonhydrogenic, while the remainder is entirely hydrogenic. It has been shown that a difference of about 0.5 is necessary to have a Cooper minimum in the continuum [37].

There is only one channel ϵp through which the electrons from the ns excited states can be promoted to the ionization continuum. The difference between the ns quantum defect and the threshold ϵp phase shift is 0.37, which is less than 0.5 therefore a minimum is expected in the discrete region

near threshold [38]. The presence of this minimum causes the ns cross section to be anomalously small at threshold [10]. The measured values of the cross section from the $4s$ 2S excited state are 1.15 Mb, 1.25 Mb, 1.03 Mb, and 0.57 Mb at 0.1 eV (near threshold), 0.7 eV, 1.3 eV, and at 2.9 eV, respectively. It is apparent that the photoionization cross section from the $4s$ excited state near the ionization threshold (0.1 eV) is lower than its value at 0.7 eV. Evidently, the photoionization cross section first increases to a maximum value of 1.25 Mb at 0.7 eV and then decreases with the decrease in the ionizing laser wavelength, deviating from the hydrogenic behavior. This confirms the theoretical prediction of Lahiri and Manson [10] about the behavior of cross sections of ns excited states of lithium.

The behavior of the photoionization cross section from the $4p$ excited state is rather different from that of the $4s$ excited state. The excited electrons from the $4p$ state can be promoted to the ionization continuum through two different channels $np \rightarrow \epsilon s$ and $np \rightarrow \epsilon d$. The contribution of $np \rightarrow \epsilon s$ channel towards the photoionization cross section is very small while the most dominating channel is the $np \rightarrow \epsilon d$ as pointed out by Lahiri and Manson [10]. The contribution of S and D waves cannot be verified on the experimental basis because experimentally we can only determine the total absolute cross section of the excited state. The threshold phase-shift difference for $np \rightarrow \epsilon d$ is only 0.5, which discards any possibility of minimum. It is clear from Fig. 5 that no minimum is present in the photoionization cross section from the $4p$ excited state near threshold. The cross sections decrease monotonically with the decrease in the ionizing laser wavelength above the first ionization threshold but this falloff of the cross section is not hydrogenic.

We have experimentally determined the photoionization cross section of the $4d$ 2D excited state from near threshold (≈ 0.3 eV) up to ≈ 3 eV above the first ionization threshold. There are two possible ionization channels, ϵp and ϵf , through which the excited electrons from the $4d$ 2D excited state can enter the ionization region. The $nd \rightarrow \epsilon p$ cross section is slightly different from hydrogenic, owing to the small p -wave phase shift, but the $nd \rightarrow \epsilon f$ is completely hydrogenic. In addition the contribution of the $nd \rightarrow \epsilon f$ channel towards the photoionization cross section is expected to be dominating over the $nd \rightarrow \epsilon p$ channel [10]. The fitted curve (Fig. 5) to the measured photoionization cross section of the $4d$ excited state decreases monotonically with the decrease in the ionizing laser wavelength, and this behavior is evidently pure hydrogenic as compared to that of the $4p$ excited state.

The calculated photoionization cross section from the $4p$ excited state at threshold is greater than the corresponding value of cross section from the $4d$ excited state as reported by Aymar *et al.* [5] and Gezalov and Ivanova [7]. Our measured value of the photoionization cross section from the $4d$ 2D excited state just above the threshold at ≈ 0.3 eV is also greater than the corresponding value of cross section from the $4p$ 2P excited state. In addition, the cross sections from the $4d$ excited state decay faster than the cross sections from the $4p$ excited state with the decrease in the ionizing laser wavelength, obeying the hydrogenic behavior. Therefore, the measured values of the photoionization cross section of the $4d$ excited state from near threshold region

≈ 0.3 eV up to ≈ 3 eV are smaller than the values of cross sections of the $4p$ excited state (see Fig. 5).

The radiative recombination is a process in which a continuum electron (free electron) is captured by an ion via a spontaneous emission of a photon. It is therefore an inverse process of photoionization. The radiative recombination process plays an important role in the measurements of the photoionization cross section near the ionization threshold. The cross section for the radiative recombination can be extracted from the detailed balance principle, as described by Lahiri and Manson [10]. A comparison of the three excited states shows that the photoionization cross sections of the $4p$ excited state are slightly greater than the cross sections of the $4d$ state but are larger by more than an order of magnitude to those of the $4s$ excited state. Accordingly, the radiative recombination cross section for the $4p$ excited state is much greater than for the $4s$ and $4d$ excited states.

IV. CONCLUSIONS

In conclusion, we have experimentally determined the absolute photoionization cross sections from the $4s$, $4p$, and $4d$

excited states of lithium, in the region from near the threshold up to ≈ 3 eV above the first ionization threshold. The energy-dependent behavior of the cross section from the three excited states of lithium has been explored for the first time. The cross sections from the $4s$ and $4p$ excited states show nonhydrogenic behavior while the falloff of the cross sections from the $4d$ excited state is purely hydrogenic, in accordance to the theoretical prediction [10]. This technique can be extended to determine the photoionization cross section as well as the photoabsorption cross section (oscillator strength) of all the alkali and alkaline earth elements. The work on the determination of absolute oscillator strength of the principal Rydberg series of lithium is in progress in this laboratory.

ACKNOWLEDGMENTS

The present work was financially supported by the Higher Education Commission (HEC), Pakistan Science Foundation (PSF), and the Quaid-i-Azam University, Islamabad, Pakistan. S.H. and M.S. are particularly grateful to the HEC for support under the Merit scheme.

-
- [1] G. V. Marr, *Photoionization Processes in Gases* (Academic Press, New York, 1967).
- [2] J. Berkowitz, *Photoabsorption, Photoionization and Photoelectron Spectroscopy* (Academic Press, New York, 1979); J. Berkowitz, *Atomic and Molecular Photoabsorption, Absolute Total Cross Sections* (Academic Press, New York, 2002).
- [3] D. E. Rothe, *J. Quant. Spectrosc. Radiat. Transf.* **11**, 355 (1971).
- [4] N. V. Karlov, B. B. Krynetskii, and O. M. Stelmakh, *Sov. J. Quantum Electron.* **7**, 1305 (1977).
- [5] M. Aymar, E. Luc-Koenig, and F. C. Farnoux, *J. Phys. B* **9**, 1279 (1976).
- [6] A. Burgess and M. J. Seaton, *Mon. Not. R. Astron. Soc.* **120**, 121 (1960).
- [7] K. B. Gezalov and A. V. Ivanova, *High Temp.* **6**, 400 (1968).
- [8] T. C. Caves and A. Dalgarno, *J. Quant. Spectrosc. Radiat. Transf.* **12**, 1539 (1972).
- [9] C. Barrientos and I. Martin, *Can. J. Phys.* **65**, 435 (1987).
- [10] J. Lahiri and S. T. Manson, *Phys. Rev. A* **48**, 3674 (1993).
- [11] K. T. Chung, *Phys. Rev. A* **57**, 3518 (1998).
- [12] S. D. Kramer, J. P. Young, G. S. Hurst, and M. G. Payne, *Opt. Commun.* **30**, 47 (1979).
- [13] V. Wippel, C. Binder, W. Huber, L. Windholz, M. Allegrini, F. Fuso, and E. Arimondo, *Eur. Phys. J. D* **17**, 285 (2001).
- [14] M. Saleem, N. Amin, S. Hussain, M. Rafiq, S. Mahmood, and M. A. Baig, *Eur. Phys. J. D* **38**, 277 (2006).
- [15] D. Hanna, P. A. Karkainen, and R. Wyatt, *Opt. Quantum Electron.* **7**, 115 (1975).
- [16] NIST database (2005), www.physics.nist.gov
- [17] R. V. Ambartsumian, N. P. Furzikov, V. S. Letokhov, and A. A. Puresky, *Appl. Phys.* **9**, 335 (1976).
- [18] K. J. Nygaard, R. E. Hebner, J. D. Jones, and R. J. Crbin, *Phys. Rev. A* **12**, 1440 (1975).
- [19] U. Heinzmann, D. Schinkowski, and H. D. Zeman, *Appl. Phys.* **12**, 113 (1977).
- [20] H. T. Duong, J. Pinard, and J. L. Vialle, *J. Phys. B* **11**, 797 (1978).
- [21] D. J. Bradley, C. H. Dudan, P. Ewart, and A. F. Purdie, *Phys. Rev. A* **13**, 1416 (1976).
- [22] A. V. Smith, J. E. M. Goldsmith, D. E. Nitz, and S. J. Smith, *Phys. Rev. A* **22**, 577 (1980).
- [23] B. Willke and M. Kock, *J. Phys. B* **26**, 1129 (1993).
- [24] W. Mende, K. Bartschat, and M. Kock, *J. Phys. B* **28**, 2385 (1995).
- [25] A. Kallenbach, M. Kock, and G. Zierer, *Phys. Rev. A* **38**, 2356 (1988).
- [26] C. E. Burkhardt, J. L. Libbert, Jian Xu, J. J. Leventhal, and J. D. Kelley, *Phys. Rev. A* **38**, 5949 (1988).
- [27] L. W. He, C. E. Burkhardt, M. Ciocca, J. J. Leventhal, and S. T. Manson, *Phys. Rev. Lett.* **67**, 2131 (1991).
- [28] C. B. Xu, X. Y. Xu, H. Ma, L. Q. Li, W. Huang, D. Y. Chen, and F. R. Zhu, *J. Phys. B* **26**, 2827 (1993).
- [29] S. Mahmood, N. Amin, Sami-ul-Haq, N. M. Shaikh, S. Hussain, and M. A. Baig, *J. Phys. B* **39**, 2299 (2006).
- [30] N. Amin, S. Mahmood, M. Anwar-ul-Haq, M. Riaz, and M. A. Baig, *Eur. Phys. J. D* **37**, 23 (2006).
- [31] N. Amin, S. Mahmood, M. Saleem, M. A. Kalyar, and M. A. Baig, *Eur. Phys. J. D* (to be published).
- [32] Shahid Hussain, M. Saleem, M. Rafiq, and M. A. Baig, *Phys. Rev. A* **74**, 022715 (2006).
- [33] K. Niemax, *Appl. Phys. B: Lasers Opt.* **58**, 147 (1985).
- [34] J. M. Song, T. Inoue, H. Kawazumi, and T. Ogawa, *Anal. Sci.* **15**, 601 (1999).
- [35] W. Demtroder, *Laser Spectroscopy* (Berlin, Springer, 1996).
- [36] J. Topping, *Errors of Observation and Their Treatment* (Chapman and Hall, London, 1962).
- [37] Z. Felfli and S. T. Manson, *Phys. Rev. A* **41**, 1709 (1990).
- [38] J. Lahiri and S. T. Manson, *Phys. Rev. A* **33**, 3151 (1986).